Astron. Astrophys. 324, 888–898 (1997)

ASTRONOMY
AND
ASTROPHYSICS

Optical emission in the radio lobes of Cygnus A⋆,⋆⋆

K. Nilsson[1], M.J. Valtonen[1], L.R. Jones[2,3], W.C. Saslaw[4,5], and H.J. Lehto[1]

[1] Tuorla Observatory, University of Turku, Väisäläntie 20, FIN-21500 Piikkiö, Finland
[2] Code 660.2, NASA/GSFC, Greenbelt, MD 20771, USA
[3] Dept of Physics, The University, Southampton SO17 1BJ, UK
[4] Astronomy Dept, University of Virginia, PO BOX 318, VA22903-0818, USA
[5] Institute of Astronomy, University of Cambridge, Madingley Road, Cambridge, CB3 0HA, UK

Received 7 November 1996 / Accepted 25 February 1997

Abstract. Deep optical imaging and spectroscopy of stellar objects in the radio lobes of Cygnus A have been carried out. Brighter optical objects close to the radio hotspots are either confirmed or suspected Galactic stars. Very faint optical emission is found coinciding with hotspot D (R $\sim$ 23.1) and hotspot B (V $\sim$ 25.4). The implications of these observations are discussed in the context of a double twin-jet model. In this model the radio lobes are assumed to contain a supermassive black hole each, and the twin jets emanating from the black holes are responsible for the radio emission. Assuming that the compact X-ray sources in the lobes arise from the accretion disks, the level of expected optical emission from the accretion disks is estimated. The present observations can rule out the model if the accretion disk is extensive, but they are not sensitive enough to exclude a truncated accretion disk, such as is expected in the slingshot ejection process. An approximate estimate for the cutoff frequency in hotspot D yields a magnetic field that is close to values obtained by other authors using minimun energy considerations.

Key words: galaxies: active – galaxies: individual: Cygnus A – radio continuum: galaxies – accretion, accretion disks

1. Introduction

Cygnus A is the best studied "classical" double radio source with two strong lobes containing plenty of interesting substructure. At the outer edge of each lobe one finds a prominent "hot spot" (hot spot A). Both lobes contain also a second hot spot (hot spot B, Hargrave & Ryle 1974) closer to the galaxy. Recently the brighter A hot spots have been called "secondary hot spots" and the less prominent B hot spots behind them "primary hot spots". This apparently contradictory nomenclature is due to a particular interpretation of the origin of the hot spots. We prefer to use the older terminology and call the secondaries A-spots and the primaries B-spots. A recent summary of the radio observations of the hot spots of Cygnus A as well as some theoretical interpretations are given by Carilli et al. (1989b) and Carilli & Barthel (1996).

The radio lobes appear to be advancing through the interstellar medium of the giant galaxy which lies approximately halfway between the two lobes. It is clear that the lobes originate from this galaxy because one of the filaments of the western radio lobe clearly connects the nucleus of the giant galaxy to this lobe (Perley et al. 1984). This filament is usually referred to as "jet". There is also some indication of another fainter filament which may connect the nucleus of the galaxy with the eastern radio lobe (see e.g. Carilli et al. 1989b).

It appears likely that the hot spot A in the western lobe is the working surface of a jet which advances into the interstellar medium, and a corresponding identification can be made in eastern lobe. The giant galaxy contains hot interstellar gas with sound speed $c_s \sim 1500$ km s^{-1} (Arnaud et al. 1984). The electron density n of this gas is relatively high, about 5.6×10^{-3} cm^{-3} even at the distance of the hot spots (R $\sim$ 90 kpc) from the center of the galaxy, but the density drops fast as a function of radius, $n \propto R^{-1}$. The working surface of the jet pushes its way through this gas at the approximate ram pressure advance speed of 3000 km s^{-1} (Carilli et al. 1991), i.e. the motion is likely to be supersonic. The radio emitting plasma flows from the A-spot and fills the lobe which is probably at a higher pressure than the surrounding hot gas (Carilli et al. 1991). The overall picture is usually connected with the twin-jet model of Blandford & Rees (1974) where a supermassive black hole in the center of the giant galaxy generates and collimates a two-sided particle flow.

The existence of the B-spot complicates the simple twin-jet picture. Evidence was presented by Valtaoja (1984) suggesting that in fact the jet which terminates at the A-spot comes from the

Send offprint requests to: K. Nilsson

⋆ Based on observations made with the Nordic Optical Telescope, La Palma, Canary Islands

⋆⋆ Based on observations made with the NASA/ESA Hubble Space Telescope, obtained from the data archive at the Space Telescope Science Institute. STScI is operated by the Association of Universities for Research in Astronomy, Inc. under the NASA contract NAS 5-26555

B-spot rather than from the center of the galaxy. This has lead to a modified view of the twin-jet model where the original jet comes from the center of the galaxy, is highly collimated, and terminates at hot spot B (Williams & Gull 1984, 1985; Lonsdale & Barthel 1986). Rather than dispersing, the jet is supposed to maintain its coherence and refocus its direction towards hot spot A. There the "bucket stops" and the proper working surface forms as in the original twin-jet model. This general type of hydrodynamics has been illustrated through numerical experiments e.g. by Williams & Gull (1984, 1985).

An alternative explanation for multiple hotspots is the "dentist's drill" model by Scheuer (1982) in which the more diffuse A -hotspots (hotspots A and D in Cygnus A, see Fig. 1) are the old jet termination points and the more compact B -hotspots are the points where the jet currently ends. This requires the jet to change its direction either by precession or by self-excited instabilities in a timescale that is short compared to the source lifetime. This kind of behaviour seems to be substantiated by the simulations of Norman (1989) and Cox et al. (1991).

Another interesting feature in the western radio lobe is the arc-like feature seen in the rotation measure map (Carilli et al. 1988). It has been interpreted as a compression zone, a bow-shock in front of a body moving inside the radio lobe. Carilli et al. (1988) argue that this body is the hot spot B even though the hot spot is clearly off the line connecting the center of curvature of the arc to the center of the galaxy. The motion of the hot spot B should deviate by about 45° from the general outward direction of the radio lobe in order to agree with the explanation. Moreover, the distance from hot spot B to the arc is an order of magnitude too large to represent the standoff distance between the bow shock and the body causing it, as Carilli et al. (1988) point out.

Kronberg et al. (1977) find no optical emission from the A-hot spots but find faint emission in the B-spot of the western radio lobe. There are several stellar objects in the lobe area, undoubtedly mostly foreground stars, but not much more is known about them.

Recently, two point like X-ray sources have been discovered in the radio lobes, one in each lobe by ROSAT (Harris et al. 1994). Their closeness to the hot spots strongly suggest that the X-ray sources are actually part of the Cygnus A system. Harris et al.(1994) dismiss the possibility that the X-ray emission is produced by thermal gas lying behind the bowshock in the ICM. Instead, the X-rays could be a result of synchrotron self-compton (SSC) emission i.e. the radio synchrotron photons are scattered to X-ray energies by inverse compton scattering by the same electron population that created the radio photons. Using Meisenheimer et al. (1989) models of particle acceleration in hot spots Harris et al. (1994) discuss the optical limits plus radio and X-ray detections which imply a dip in the spectrum in the optical, and a subsequent rise again into the X-ray. In contrast, the Meisenheimer et al. (1989) model involves power-law spectra which are monotonically decreasing functions of frequency. If the X-rays are to be of synchrotron origin, then there must be a mechanism which produces only the highest energy electrons, but avoids producing optically emitting electrons, i.e. the electron spectrum should be double peaked with one peak at radio emitting energies and a second at X-ray emitting energies. Hence the conclusion of Harris et al. (1994) that the X-rays are not sychrotron in origin but due to the inverse Compton mechanism.

Reynolds & Fabian (1996) have also detected the X-ray emission from the western hotspot region in the ROSAT PSPC 0.5 – 2.0 keV band. Their spectral analysis implies $\alpha \gtrsim -0.7$ ($S_\nu \propto \nu^\alpha$) for the eastern hotspot in the 0.5 –2.0 keV band. This is slightly harder than what Harris et al. (1994) predict in their SSC model.

There is an alternative explanation of the double hot spots in radio lobes. In this view there are actually two working surfaces of jets in each lobe, one jet terminating in hot spot A and the other in hot spot B. This requires that the supermassive black hole responsible for the jets lies between the two hot spots. Supermassive black holes flying out of galaxies are not difficult to understand (see e.g. Mikkola & Valtonen 1990, Valtonen et al. 1994); rather it would be difficult to understand if they were always bound to the centers of galaxies (Valtonen 1996a, b). In multiple mergers of galaxies, now thought to be common (see e.g. Kauffmann & White 1993), multiple systems of supermassive black holes are gathered together. Due to the instability of such systems the black holes are thrown out of galaxies. An important mode of instability is the ejection of black holes in opposite pairs for which Cygnus A could be a typical example: the escape speed of 3000 km s^{-1} from the galaxy and the ratio of distances of the two black holes from the center of the galaxy of 1.1 are not unusual for the ejected black hole pairs (Valtonen et al.1994).

We will consider the simple case of a free jet which flows out from the black hole into a conical volume. Let the jet flow speed be v_J and the distance from the black hole along the jet r. Then the pressure in the jet

$$P_\mathrm{J} \propto v_\mathrm{J}^2 r^{-2}. \quad (1)$$

The jet flow will terminate when it is opposed by an equal pressure, either the ram pressure

$$P_\mathrm{R} = \rho_0 v_0^2 cos^2\alpha \quad (2)$$

of the external medium or the thermal pressure

$$P_\mathrm{T} = 3/5\rho_\mathrm{s} c_\mathrm{s}^2. \quad (3)$$

Here ρ_0 is the density of the interstellar medium which the jet meets. The velocity of advance of the black hole is v_0 and the jet lies at an angle α relative to the line of motion. The sound speed of the medium is c_s and its density is ρ_s. The latter density refers to the shocked medium in case one of the jets terminates inside this medium and is not confined by the ram pressure.

The condition for ram pressure confinement is thus $P_\mathrm{J} = P_\mathrm{R}$ or $v_\mathrm{J}^2 r^{-2} \propto \rho_0 v_0^2 \cos^2\alpha$. This gives the jet length of

$$r_\mathrm{J} \propto (v_\mathrm{J}/v_0)(\cos\alpha)^{-1}\rho_0^{-1/2} = r_\mathrm{proj}/\cos\alpha, \quad (4)$$

where $r_\mathrm{proj} = (v_\mathrm{J}/v_0)\rho_0^{-1/2}$ is the projection of the jet to the direction of motion. In different parts of the jet cone α is

different but r_J varies in such a way that its projection to the line of motion is constant. In other words, the jet terminal surface is at right angles to the line of motion. As far as we are dealing with free jets, this fact may be used to determine the current direction of motion of the black hole.

In case the jet is terminated by isotropic thermal pressure, $v_J^2 r^{-2} \propto \rho_s c_s^2$ or

$$r_J \propto (v_J/c_s)\rho_s^{-1/2} \quad (5)$$

and the terminal surface is at right angles to the center line of the jet. However, in general we may expect pressure gradients in the shocked medium of the lobes. We get an idea of such a pressure distribution by looking at the hydrodynamic simulation of De Young (1977). In this simulation De Young considered a lobe which is formed by a high pressure source of plasma moving through the interstellar medium. The source could be either a black hole or the terminal point of a beam from the center of the radio galaxy. In the front of the lobe (hot spot A) the pressure is indeed as expected from the shock, while the pressure drops when going back along the lobe such that the pressure is higher along the edges of the lobe than near to its central axis.

The discussed jets are not inconsistent with the first-order Fermi acceleration theory and its application to radio hot spots. In this theory the jet speed u_j is given by

$$u_j \approx 0.008c\,(B/10^{-4}\mathrm{G})^{3/2}(L/\mathrm{kpc})\left(\frac{\nu_b}{\mathrm{GHz}}\right)^{1/2} \quad (6)$$

(Meisenheimer et al. 1989, Eq. 11). Here ν_b is the frequency of the spectral break where the power law index α ($S_\nu \propto \nu^\alpha$) changes from -0.5 to -1.0, B is the magnetic flux density in the hot spot, and L is the thickness of the emission region. Here we have assumed that the spectral cutoff frequency $\nu_c \gg \nu_b$ which seems to be true in the A hot spots of Cygnus A. If we use the parameter values from Muxlow et al. (1988) $\nu_b \approx 2$ GHz, B $\approx 4 \times 10^{-4}$ G and L ≈ 1.1 kpc, we obtain $u_j \approx 0.1$ c. However, the magnetic flux density B may be well below the equipartition value mentioned above. A factor of three reduction in the magnetic flux density below the equipartition value which was found by Carilli et al. (1991) for the lobes would bring the jet speed down by a factor of five. The jet speed relative to the interstellar medium should be higher in the forward direction and lower in the backward direction, if the speed of the black holes through the interstellar medium is a significant fraction of the jet speed relative to the black holes.

The so called "jet" of Cygnus A is a bright filament which was originally thought to be overpressured relative to the lobe medium (Perley et al. 1984). However, it lies closer to the center of the galaxy than the heads of the lobes and is therefore at higher confining pressure by about a factor of two than the outer parts of the lobes (Arnaud et al. 1984). Using the models of Carilli et al. (1991) we then estimate the pressure surrounding the jet as 4×10^{-10} dyn cm^{-2}. Perley et al. (1984) quote the same number as the minimum pressure of the faint jet. Thus it is possible to view the jet as a relatively stable magnetic field structure inside the lobe, a trail of the B hot spot (Valtonen 1979). Begelman & Cioffi (1989) have also reached the same conclusion as far as the pressure confinement of the jet is concerned.

The jet has now been imaged at resolutions ranging from 0.1 milliarcsec to 1 arcsec and it shows a remarkable continuity from scales less than 0.2 pc to scales grater than 10 kpc, inspite of the 5-15° bend in projected direction between these scales (Krichbaum et al 1993). Also direct measurements of outward motion of knots in the innermost jet have been obtained, indicating an apparent jet velocity of about one third of the speed of the light (Carilli et al. 1994). In the slingshot model one assumes that the jets from the central black hole are diverted to the pre-existing ejection trails where they are bent by magnetic fields (Koide et al. 1996). This may give the apparence of the jet continuing as far as the outer filament. A filament may also serve as an efficient channel of particle propagation and may in this sense be viewed as a real continuation of the central jet. The connection between the central black hole and its jets with the ejection channels is discussed further by Valtonen (1996).

There is a simple way either to prove or disprove this modification of the twin-jet model. One should look for signs of a black hole and an accretion disk surrounding it in the radio lobes (Rees & Saslaw 1975). The black holes should lie close to the line connecting the two hot spots and they should in most cases be observable in X-rays. Therefore it would be very important to locate the point sources seen in the lobes by ROSAT more accurately. The crucial test of this theory comes from the search for the optical evidence for the accretion disks in the radio lobes.

Using the existing accretion disk models, one may estimate the optical brightness of such a disk. For this purpose we will use the models of Wandel & Petrosian (1987,1988) which contain a geometrically thin accretion disk surrounding the central black hole with the main parameters being the mass of the black hole (M), the accretion rate onto it ($\dot{m}$) and the viscosity parameter α (viscosity $\propto \alpha P_{tot}$; P_{tot} = total pressure in the disk) or β (viscosity $\propto \beta P_{gas}$; P_{gas} = gas pressure in the disk). The luminosity and spectral shape of the accretion disk emission are mainly determined by M and $\dot{m}$. The local emitted spectrum of the outer parts of the disk has a shape of a blackbody spectrum at the local surface temperature and the total emitted spectrum can be calculated by summing the blackbody spectra at different radii. The effect of electron scattering, comptonization and the change from an optically thick to an optically thin region have to be taken into account in the inner parts of the disk. These effects can modify the spectrum from a pure blackbody emission significantly. Wandel & Petrosian (1988) calculate the expected luminosity and spectral slope of an accretion disk in the optical and UV regions in a grid of different central black hole masses and accretion rates. Since the accretion disks are truncated by the ejection process (Lin & Saslaw 1977), we have to modify the calculations to include only the central parts of the disk model. These models are discussed more in Sect. 4 after we present the observations.

Every double lobed radio source imaged with sufficient resolution and sensitivity always shows compact, flat spectrum radio emission from the central engine. One may wonder why in

Table 1. Log of optical observations at the NOT

Date	Detector	Band	Component (east/west)	Exp. time (s)	FWHM (arcsec)	Notes
23 Aug 1993	Stockholm	V	west	837	0.64	photometric, $k_R = 0.14$
	CCD	R		837	0.57	
		I		879	0.56	
1 Jul 1994	Stockholm	B	east	1799	0.88	mostly photometric, $k_R = 0.14$
	CCD	V		902	0.79	variable extinction at the end of the night
		R		6129	0.79	
		I		902	0.90	
2 Jul 1994	Stockholm	B	west	2998	1.24	variable extinction
	CCD	V		902	1.10	$k_R = 0.15 - 0.50$
		R		2104	0.84	
7 Jul 1994	IAC CCD	R	east+west	12000	0.97	very high but stable extinction, $k_R = 0.66$

Cygnus A there is no evidence of compact, flat spectrum radio source in the vicinity of the hotspots at any frequency, including VLA imaging at 8, 15 and 22 GHz at resolutions of 0.2, 0.1 and 0.05 arcsec (Perley & Carilli 1996, Carilli et al. 1989b, Perley et al. 1997). Hence, the hypothesized black hole + accretion disk at the end of each lobe must be relatively quiet in radio.

In the accretion disk models of Wandel & Petrosian (1988) the disk radio emission is low. If these models are generally applicable to galactic nuclei, the compact flat spectrum emission must come from other mechanisms than was considered by Wandel & Petrosian (1988). Possible alternatives are e.g. the emission from the magnetospheres of the disks or from the inner parts of the jets. The appearance of this radio emission is strongly dependent of the optical depth of the source. The reason why the radio emission should come more efficiently from the ends of the jets when the black hole is outside the nucleus than when it is in the nucleus of the galaxy is not clear. However, there are many potential differences such as different magnetospheric structures and a different optical depth considering the vastly different environments of stationary black holes in the dense nuclei of galaxies and the rarefied environment in which the ejected black hole travels. Because of this uncertainty in the generation of radio emission in the vicinity of the black hole we consider other wavebands more promising in testing the ejected black hole hypothesis.

2. Observations and data reduction

2.1. Optical imaging

Cygnus A was observed during four observing sessions at the Nordic Optical Telescope (NOT) on La Palma during 1993 and 1994. Table 1 gives the log of observations. The main part of the observations comes from July 1994 when three nights were devoted to deep BVRI imaging. The integration times of individual exposures varied between 120 and 600 seconds depending on the filter used. Between the exposures the telescope was moved in steps of a few arcsec. On July 1 and 2 we used the Stockholm CCD camera, which has a TEK 512 × 512 detector with a pixel size of 0.1965 arcsec, a gain of 8.5 electrons ADU^{-1} and a readout noise of 19.6 electrons. The field size of this camera is 100 arcsec. Since the angular size of Cygnus A is 120 arcsec, the lobes had to be imaged separately. The Stockholm CCD was used also in September 23 1993 when the Western lobe was imaged under excellent seeing conditions. On July 7 1994 we used the IAC CCD camera equipped with a TEK 1024 × 1024 detector with a pixel size of 0.14 arcsec, a gain of 2.0 electrons ADU^{-1} and a readout noise of 5.4 electrons to obtain a very deep R-band image of Cygnus A. The field size was 143 arcsec, which made it possible to capture the whole object in one exposure.

Table 2. Log of spectroscopic observations obtained at the WHT with the ISIS spectrograph. The object names refer to those in Fig. 2

Date	Object	Exp. time [s]	slit width [arcsec]	FWHM [arcsec]
1 Jul 1994	E3	3600	1.0	0.9
21 Jun 1993	W3	900	1.5	1.0
17 May 1994	W4	3000	1.0	0.8
17 May 1994	W5	3000	1.0	0.8

Standard stars from Landolt (1983) and Landolt (1992) were observed each night to obtain the photometric calibration. The last column in Table 1 gives comments on the photometric quality of the nights based on the examination of the magnitudes of standard stars and the stars in Cygnus A fields. The R-band exposures of Cygnus A were distributed throughout the night and thus provide a way to check if the extinction was changing during the night. The observations of July 1994 were affected by an increasing amount of Sahara dust in the atmosphere towards the end of observing run. The night of July 2 is the one mostly affected by the dust in form of variable extinction.

The IRAF package was used to bias subtract and flat-field the images with twilight flats in the standard way.The individual images in all bands were registered and combined and cleaned of cosmic ray events. For astrometric calibration of the field we used the APM Northern Sky Catalogue (Irwin et al. 1994) which is a digitized version of the Palomar sky survey. We measured the positions of 25 stars in the deep R-band field from July 7 1994 to obtain the transformation from pixel positions to

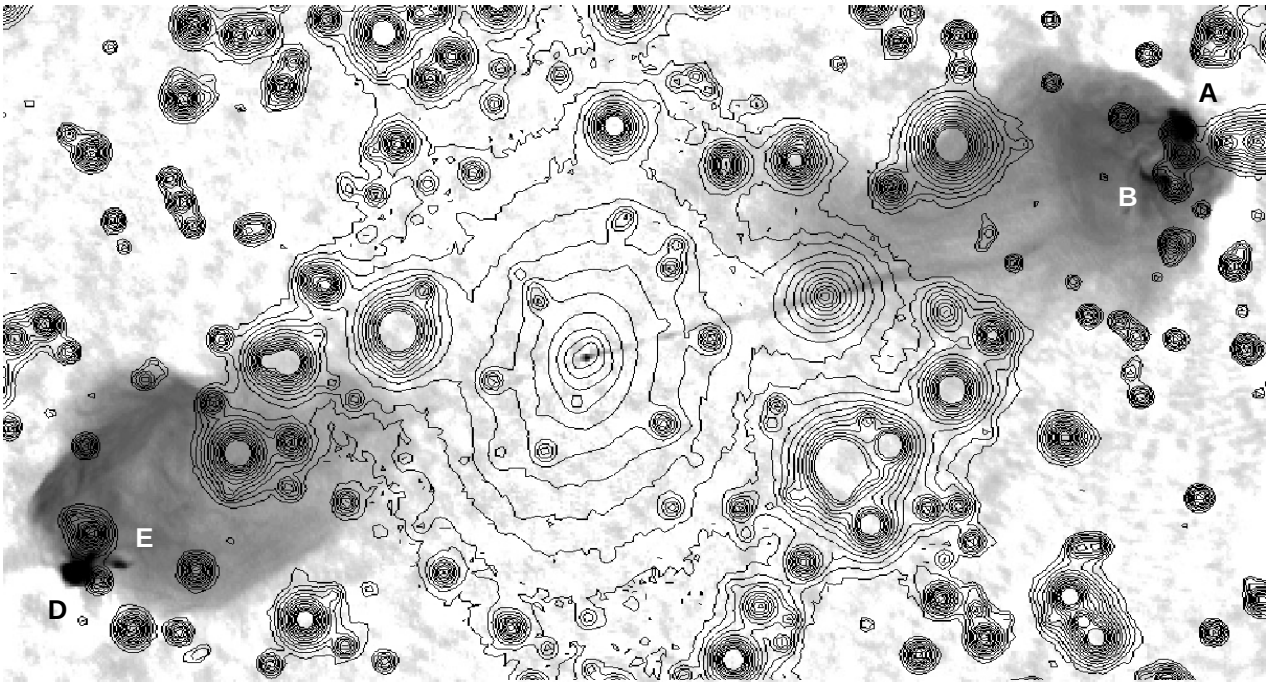

Fig. 1. The 8.5GHz radio image (greyscale) of Cygnus A overlaid by the contours of the combined R-band image from the observations of July 7 1994. The radio hotspots, designated A, B, D and E (Hargrave & Ryle 1974), have been marked in the figure. Lowest contour corresponds to 23.5 mag/square arcsec, the contour interval is 0.5 mag/square arcsec. The field size is 143 × 73 arcsec. The radio image is by courtesy of R. Perley and the Cygnus A CD-ROM project.

equatorial coordinates. The residuals of our fits have a standard deviation of 0.25 arcsec in both right ascension and declination, consistent with the internal accuracy (0.1 – 0.25 arcsec depending on the brightness of the object) given by Irwin et al. (1994). The external accuracy of the catalogue is $\sim$ 0.5 arcsec.

2.2. Spectroscopy

Spectra for four objects in the outer lobes of Cygnus A were obtained at the William Herschel Telescope, La Palma using the red and blue arms of the ISIS spectrograph (Clegg et al. 1992). Table 2 gives the log of observations, which were obtained partly in RGO service time. The frames containing the spectra were de-biased, flat-fielded and background subtracted in a standard way. The spectra were extracted, combined and wavelength calibrated using calibration lamp exposures made between the exposures on the targets. Flux calibration was achieved via spectra taken of spectrophotometric standard stars temporally close to the target exposures. The resulting spectra cover a wavelength scale from 3800 Å to 9000 Å with a FWHM resolution of 6 – 7 Å and a dispersion of 3 Å / pixel.

3. Results

Fig. 1 shows the 8 GHz radio image (in greyscale) overlaid by the contours of the combined R-band image of the Cygnus A field from the observations of July 7 1994. Several stellar objects can be seen close to the radio hotspots, especially in the western lobe. Fig. 2 shows the optical surroundings of the radio hotspots in more detail. The upper panels are cut from the R-band image of July 7 1994 which is a median combined image of 40 exposures with a total exposure time of 12 000 seconds. The limiting magnitude, which we define as the magnitude of the faintest object measureable with better than 3 sigma accuracy using aperture radius of 0.75 FWHM ($\sim$ optimal aperture, Howell 1992), is about 24.4 in this image (without the presence of excessive amounts of dust in the atmosphere a limiting magnitude of $\sim$ 0.7 mag deeper would have been attained). The optical objects around the radio hotspots have been labeled with numbers and in all following discussion we refer to e.g. object 2 in the eastern field as "object E2".In the upper right panel of Fig. 2 we have also sketched the position of the rotation measure arc discovered by Carilli et al. (1988). All panels have been overlaid by the 8 GHz radio contours.

The lower panels of Fig. 2 show the same fields as the upper ones, but in these panels the brighter objects around hotspots have been subtracted using a PSF constructed from field stars. Dots denote the positions where a subtraction has been performed (Object 2 in the western lobe has not been subtracted for better comparison with the radio emission). The images have been smoothed with a Gaussian core and contrast has been enhanced to show the faint objects more clearly. The square boxes show the positions of the X-ray emission determined by Harris et al. (1994) by aligning the center of the optical galaxy with the central peak of the X-ray emission. The sizes of the boxes indicate our estimated error between X-ray and radio/optical positions (Harris et al. 1994 estimated their positional uncertainty

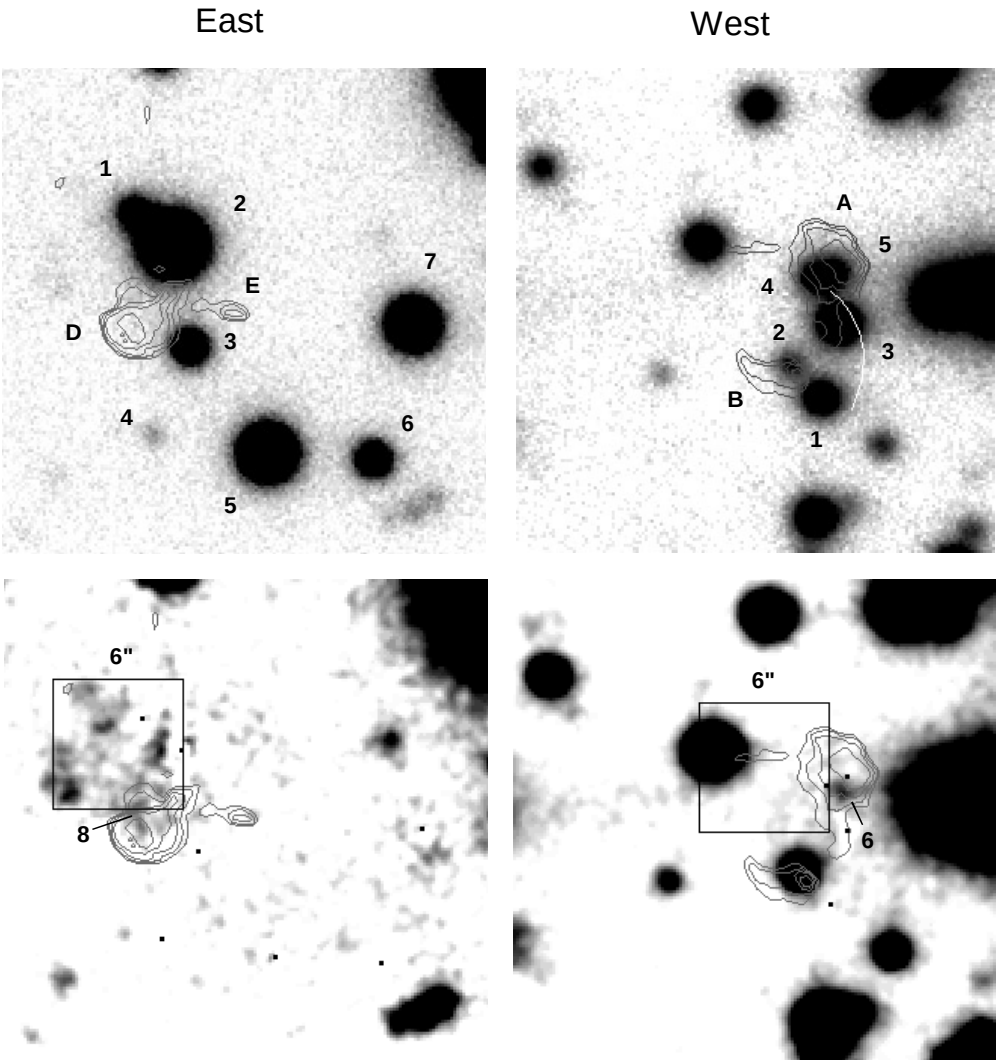

Fig. 2. A montage showing the optical field around the radio hot spots of Cygnus A in the eastern and western lobe. The field size is 22.5 × 22.5 arcsec in each panel, north is to the up and east is to the left. *Upper panels* show 12 000 seconds of exposure in the R-band from July 7 1994. The 8 GHz radio contours of the hotspots have been overlaid and optical objects labeled. The white arc in the western lobe indicates the position of the rotation measure arc detected by Carilli et al. (1988). *Lower panels* show the same fields after subtraction of brighter optical objects (except object 2 in the western lobe) and smoothing with a gaussian kernel. Dots indicate the positions where a subtraction has been performed. Additional faint objects are revealed in both lobes. The boxes give the position of the X-ray spots from Harris et al. (1994) with our estimated positional error with respect to radio-optical reference frame.

to be 2″ to which we have added our uncertainty of measurement from their Fig. 1). The relative positions of radio and optical to each other are determined to a much better accuracy, about 0.7 arcsec. Harris et al. (1994) show that the peaks of the X-ray emission are spatially coincident with the peaks of the radio emission in the lobes in a 1.45 GHz map with 7.5 arcsec resolution. The latter resolution is too low to pinpoint the hotspots accurately; at this resolution the position of the maximum brightness is strongly affected by the general lobe emission in addition to the hotspots.Thus even though the X-ray positions are within 2″ of the bright spots in the 1.45 GHz radio map, they lie further than 2″ from the radio hotspots at the 8.5 GHz map.

From the point of view of the double twin-jet model objects E3 and W3 were the first candidates for a black hole to be checked since they lie close to the line connecting the radio hotspots. Object W3 would also be projected in the right place to be the cause of the bow shock giving rise to the rotation measure arc. These two objects were selected as the primary targets for our spectroscopic studies. In the Eastern lobe none of the brighter objects is coinciding with the radio hotspots whereas in the western lobe objects W4 and W5 lie very close to hotspot A and object W2 almost coincides with hotspot B as was already noted by Kronberg et al. (1977). A spectroscopic study of also these objects is desirable, but due to the observing time constraints, we were able to obtain a spectrum of the objects W4 and W5 only.

After subtraction of the brighter objects two fainter objects E8 and W6 can be seen. Object E8 is diffuse and nearly coincides with hotspot D. It has approximately the same shape and size as the radio hotspot indicating that it could be optical synchrotron radiation arising from the same radiation process as the radio emission. The flux inside an aperture of diameter 2.8 arcsec and centered on E8 corresponds to a magnitude R = 23.1 ± 0.2. There are several faint objects towards NE from E8, which look like faint stars or members of a distant group of galaxies. It cannot therefore be ruled out that E8 is a member of a group of background or foreground objects unrelated to the radio emission. A much stronger case for the synchrotron origin of object E8 would be made by showing that the emission from E8 is linearly polarized. Although only a handful of polarization observations of optical hotspots have been published, the general trend seems to be that the degree of polarization in

Table 3. The Hubble Space Telescope archive images used in this work.

Date	Field (east/west)	Exp. time [s]	Filter
18 Mar 1994	east	600	F622W
		600	
		600	
18 Mar 1994	east	600	F450W
		600	
		600	
09 Sep 1994	west	900	F555W
		900	
		900	

these objects is rather high (e.g. 29 % in 3C 33, Meisenheimer & Röser 1986 and 46 % in Pictor A, Röser 1989). The faintness of object E8, however, makes polarization measurements of this object possible only at the very largest telescopes.

In the western lobe, a very faint object W6 is seen after subtraction. Objects W4-W6 all lie within 1.1″ from each other thus making it difficult to distinguish the objects from each other. However, object W6 appears clearly also in the V, R, and I images of September 1993 taken under excellent seeing conditions. We therefore consider object W6 to be a real feature. Unlike object E8 it appears stellar in all images.

We have also looked for optical images of the region around the outer lobes of Cygnus A in the Hubble Space Telescope archive. We found 6 images of the Eastern field and 3 images of the western field obtained with the WFPC2. Table 3 gives the details of the images. The images in each filter were combined for comparison with our ground-based images. Fig. 3 shows the optical field around the western lobe through the F555W filter. In addition to objects 1-6, a very faint object, labeled 7, can be seen. This object coincides exactly with the radio hotspot B and thus very likely represents the optical tail of the synchrotron radiation from hotspot B. As with E8, optical polarimetry should be made to confirm the identification. We measured the magnitudes of objects W1–W3 in the HST image and compared these values to our V-band magnitudes of the same objects. The magnitude differences had a standard deviation of 0.02 mag with no obvious dependence on object color. This simple photometric calibration yields V = 25.4 $\pm$ 0.3 for object W7. There is also a hint of diffuse emission towards N and NE of objects W4–W6 in the western lobe. This emission is better visible when one subtracts objects W4–W6, but it is still at the edge of detectability. In the Eastern field, a very faint diffuse region of emission is seen at the location of E8 in the combined image taken through F622W filter. The diffuse appearance of this object contrasts with the objects towards N and NE from E8, which appear stellar in the HST images. The fact we can see E8 both in the NOT and the HST data gives us confidence that this feature is real. The reality of the faint emission region in the western lobe should be checked with deeper observations.

Fig. 4 shows the spectra of the four selected targets. Several stellar absorption lines can be identified and the spectra look like those of an F and G-type star with W3 and E3 being of earlier type (the G-band is absent or weak in these) and W4 and W5 of later type. Note that since W4 and W5 lie only $\sim$ 1 arcsec away from each other, they were barely resolved and some light is leaking from W4 to W5. The spectrum of E3 shows some spurious features at 5000 - 5200 Å and 6700 Å which are not real but due to the reduction process.

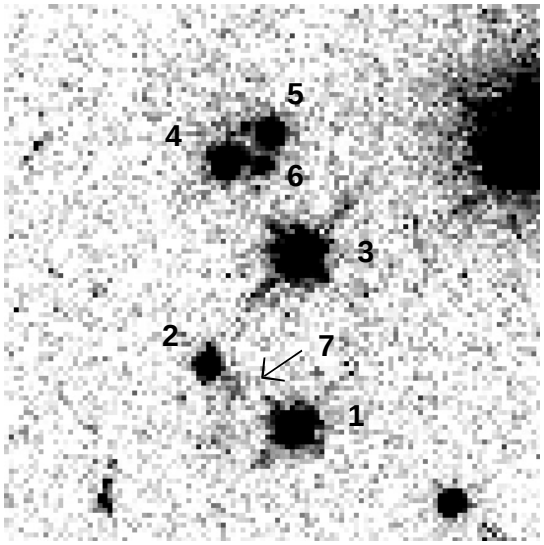

Fig. 3. The Hubble Space Telescope image of the western field of Cygnus A through the F555W filter. The labelling of the objects 1–6 is the same as in Fig. 2. Object 7 (arrowed) coincides with radio hotspot B. The field size is 10.5 $\times$ 10.5 arcsec, north is up and east is to the left.

Table 4. Results of photometry of optical objects near the radio hotspots.

East/ West	object	R_c	(B – V)	(V – R_c)	(V – I_c)
East	1	20.4 $\pm$ 0.1	1.3	0.6	1.1
	2	17.6 $\pm$ 0.1	1.0	0.6	1.1
	3	19.9 $\pm$ 0.1	1.2	0.6	1.1
	4	22.6 $\pm$ 0.1	-	$>$ 1.3	$>$ 2.9
	5	18.2 $\pm$ 0.1	1.0	0.6	1.1
	6	20.0 $\pm$ 0.1	1.8	1.0	1.8
	7	18.6 $\pm$ 0.1	1.1	0.7	1.2
	8	23.1 $\pm$ 0.2	-	-	
West	1	19.8 $\pm$ 0.1	1.0	0.5	1.1
	2	21.1 $\pm$ 0.1	1.4	0.9	1.7
	3	19.2 $\pm$ 0.1	0.9	0.5	1.0
	4	20.2 $\pm$ 0.1	0.9	0.6	1.2
	5	21.0 $\pm$ 0.1	1.4	0.7	1.4
	6	22.8 $\pm$ 0.3	-	0.9	1.9

Photometry was also done on the objects visible in the NOT images. For this purpose we used DAOPHOT (Stetson 1987) implemented in IRAF. The magnitudes were measured by fitting the PSF to the core region (typically the region inside 1 – 1.5 FWHM radius) of the objects. With close groupings of objects, such as W4–W6, we used the DAOPHOT's ability to fit groups of objects simultaneously. The results of the photom-

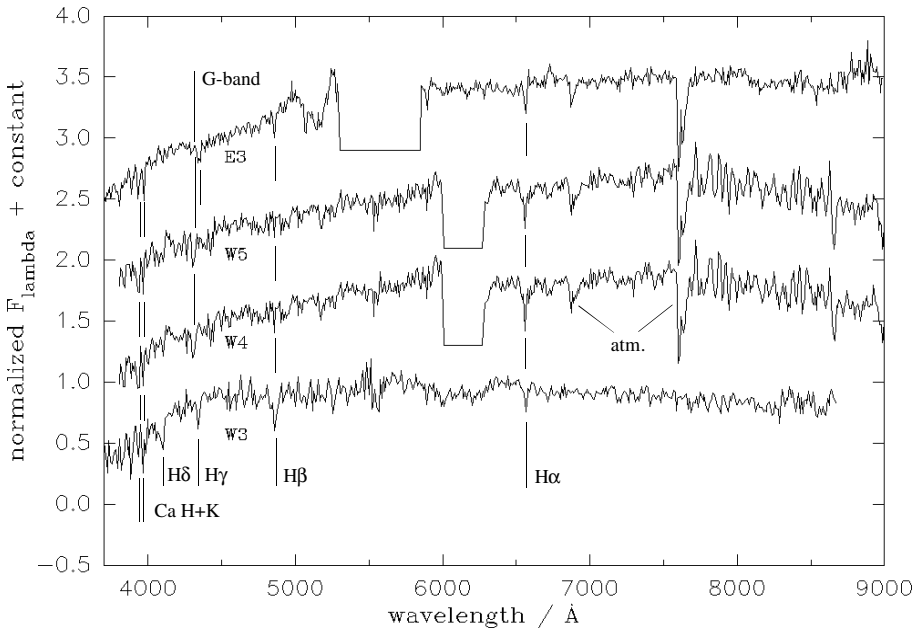

Fig. 4. Spectra of the selected targets in the outer lobes of Cygnus A. The spectra have been normalized to F_λ(6400 Å) = 1.0 and a constant (0.8) has been added to separate the spectra. The most prominent spectral features are also marked. Gaps in the spectra are due to the dichroic mirrors in the ISIS spectrograph.

etry are given in Table 4. The magnitudes have been rounded to nearest 0.1 mag since this is the accuracy at which the measurements made with different detector and filter combinations and in varying atmospheric conditions agree with each other. The main source of uncertainty in our observations comes from the determination of the photometric zero points and extinction coefficients. The noise from photon statistics and background determination was usually much smaller than 0.1 mag except for the very faintest objects. In these cases the error from the photon statistics has been incorporated into the error estimates.

The results of the photometry are summarized in Fig. 5 where we plot the V–R color of the objects against V–I color. In the same figure we also show the location of main sequence stars of different spectral types. The colors of main sequence stars (as well as all zero magnitude fluxes used in this paper) are from Bessell (1979). The figure also shows an arrow displaying the direction and maximum extent of reddening the objects could experience in the direction towards Cygnus A (assuming uniform extinction towards it). The extinction at different wavebands was calculated using A_V = 1.26 (Harris et al. 1994 and references therein) and the average interstellar extinction curve by Savage & Mathis (1979).

The colors of the objects presented in Table 4 and in Fig. 5 are consistent with colors of galactic main sequence stars with the actual spectral class depending on how much the reddening is affecting the colors. The same conclusion is reached by examining the B–V color against the V–I color. Judging from the objects observed spectroscopically, the stars in the outer lobes of Cygnus A seem to be reddened by approximately the same amount as the Cygnus A galaxy.

4. Discussion

4.1. Black holes in the lobes of Cygnus A?

At this point we may ask what kind of colors and magnitudes would be expected if there were black holes in the outer lobes of Cygnus A. Here we have to restrict ourselves to crude estimates only since the accretion phenomenon is not well understood yet. For instance, it is not clear if there is more than just one emission component contributing to the total emission (e.g. the "hot" and "cool" disks of Wandel & Liang 1991) and how they are located with respect to each other ("sandwich" or radial geometry). We will assume that the emission coming from the black hole is pure accretion disk radiation without the need to consider any additional emission components as in the case of quasar or Seyfert spectra (see e.g. Thompson 1995). Furthermore, we do not have any *a priori* information of the accretion rate or the mass of the ejected black hole, since the physical conditions surrounding the ejected black holes are expected to be very different from those in galactic nuclei. Thus it may be that the part of M – $\dot{m}$ parameter space studied by Wandel & Petrosian (1987,1988) is not relevant to our case.

Wandel & Petrosian (1987) calculate the luminosity and spectral index between 4200 Å and 7500 Å of an accretion disk around a black hole for different central black hole masses and accretion rates. At the redshift of Cygnus A these wavelengths have shifted close to the effective wavelengths of our B(4400 Å) and I(7900 Å) filters. We have therefore used the observed B and I magnitudes to calculate the spectral slope between 4200 Å and 7500 Å. Here we will not be able to take advantage of the full BVRI photometry since optical colors for all bands were not calculated by Wandel & Petrosian (1987) and anyway they depend on the details of the model (see e.g. Fig. 1. of Wandel & Petrosian 1988). The B–I color on the other hand is sensitive to the location of the peak of emission which in turn depends on M and $\dot{m}$.

High accretion rates in this model ($\dot{m} \gtrsim 10$; $\dot{m} = 4.4(\dot{M}/M_\odot$ $yr^{-1})(M/10^8\ M_\odot)^{-1}$ = 17.5 L/L_{Edd}) with high black hole masses ($M \sim 10^8 - 10^{10}\ M_\odot$) can immediately be excluded by our data. In this case flat or inverse spectra ($\alpha^{7500Å}_{4200Å} \sim$ -0.2 –

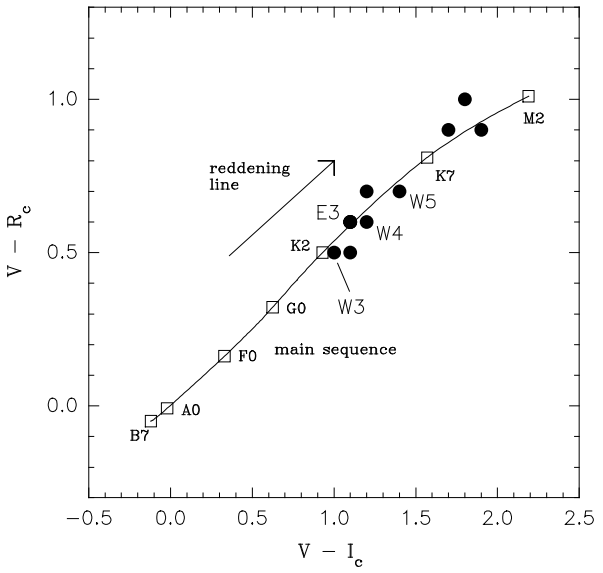

Fig. 5. Comparison of the observed colors of optical objects in the lobes of Cygnus A (filled circles) with colors expected from galactic stars. The objects observed spectroscopically are labeled.

1.0; $F_\nu \propto \nu^\alpha$) in the optical regime and B-magnitudes of ~ 8 – 15 are expected (see Fig. 3 of Wandel & Petrosian 1987). The objects observed in the lobes of Cygnus A are clearly fainter and redder ($\alpha \sim$ -0.4 – -3.2, most objects have α equal to -0.9) than this even if one assumes that they experience the same amount of extinction as Cygnus A.

Fainter magnitudes and red colors are possible when both M and $\dot{m}$ are lower that quoted above. For instance, a black hole with M = 10^8 $M_\odot$ and $\dot{m}$ = 0.01 would have a B-magnitude of ~ 20 and a B–I color of ~ 3.0, which is in the range of observed values, 19.2 – 23.4 and 1.9 – 3.6, respectively. There are thus parts in the M – $\dot{m}$ -plane where we could in principle mistake a black hole for a galactic star if we look at the B-magnitude and B – I color only. In these cases, however, the derived accretion rates would be too low to account for the observed X-ray emission. If we assume that the accretion rate is high enough for significant X-ray production ($\dot{m} \gtrsim 10$ in previous units), use the observed X-ray brightness and assume that the spectrum from optical to X-ray frequencies has a ν^{-1} dependence (Wandel & Petrosian 1988) we should expect an optical brightness of B ~ 21.5. This is close to the brightness of some of our objects but the spectra and the BVRI-colors give us no reason to suspect them to be anything but galactic stars. All optical emission brighter than V ~ 25.4 in the western lobe and R ~ 24.4 in the eastern lobe thus seems to come from galactic objects or to be associated with the radio hotspots and no signs of an accretion disk at this level are seen. For an accretion disk to remain undetected the optical to X-ray spectral index would have to be $\gtrsim -0.6$ in both lobes. The mass of the black hole would have to be relatively low in order to account for the low level of optical emission. Comparing the optical upper limits to the figures of Wandel & Petrosian (1987,1988) shows that M would have to be $< 10^5$ – 10^6 $M_\odot$ if one wants to keep the accretion rate high enough for significant X-ray production. An estimate for the lower limit of the black hole mass can be obtained from the fact that the black hole has to be able to power the radio hotspots. The radio luminosities of the hotspots are $\sim 2 \times 10^{44}$ erg s^{-1} in both lobes. This requires a minimum of 0.06 $M_\odot$ per year to be deposited into the black hole, which would then have to have M $> 3 \times 10^6$ $M_\odot$ to be able to produce X-rays.

So far we have assumed that the accretion disks survive the tidal forces in close encounters between black holes in the center of the galaxy before the ejection takes place. Lin & Saslaw (1977) have studied a case where a single black hole passes close by a binary black hole with a sufficiently low impact parameter for an ejection to happen. The single black hole and the binary are both in turn "dressed" with an accretion disk which is modelled by test particles that move around the black holes in Keplerian orbits and their evolution is followed during the encounter with numerical calculations. Lin & Saslaw (1977) found out that the accretion disks have the best chance to survive the encounter when the single black hole has the same mass as the binary and the ejection is symmetric. This is also the most relevant case to double radio galaxies which tend to have their arm length ratios close to unity (e.g. Best 1996). Even in the case of nearly symmetrical ejection the outer parts of the disks are stripped away with the actual amount of disruption depending on the mass ratio of the single black hole and the binary and on geometry of the encounter. The disruption of the outer parts of the disk can have a significant effect on the observed spectrum. The cooler, outer parts of the disk which contribute most in the optical region can be thrown away leaving only the X-ray emitting inner parts. This could account for the lack of optical emission in the lobes of Cygnus A and consequently the black hole could have higher mass and still remain undetected. The maximum extent of the accretion disks around ejected black holes is about 100 Schwarzschild radii. The spectral index between optical and X-rays coming from the central 100 Schwarzschild radii in the models of Wandel & Liang (1991) is in the range of -0.3 – -2.0. Assuming that the observed X-ray emission comes from the truncated accretion disk, the expected optical brightness could be about 2 magnitudes below our detection limit.

Neither is optical line emission expected in the very hot truncated disk. Even if it had cooler line emitting regions embedded in it, the very high rotation speeds around the black hole would broaden the lines and make their separation from the continuum difficult. Carilli et al. (1989a) derive the upper limit of 2.3 $\times$ 10^{-5} erg cm $^{-2}$ s^{-1} sr^{-1} for the H_α/N[II] line emission in the radio lobes, but because the lines in the accretion disk can be very broad, it is difficult to constrain the line flux with these observations.

The implied total accreted mass (assuming source lifetime of 10^7 years, Carilli et al. 1991) is greater than 10^6 $M_\odot$. Obviously the black hole has to carry all this matter with it during the ejection process and after the ejection. Typically the mass of the accretion disk is a large fraction of the mass of the black hole, but there is no problem at least dynamically for the truncated disk to follow the black hole (Lin & Saslaw 1977). The ejected black hole will lose its power when it has exhausted its accretion

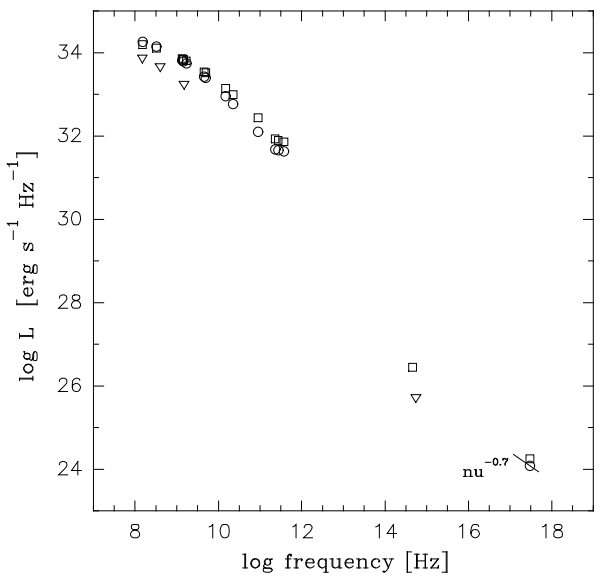

Fig. 6. The broadband spectra of hotspots A (circles), B (triangles) and D (boxes). The radio data are from Carilli et al. (1991) and Muxlow et al. (1988) and the X-ray data are from Harris et al.(1994). The line crossing the X-ray data point of hotspot A indicates the lower limit of spectral index ($\alpha > -0.7$; $S_\nu \propto \nu^\alpha$) in the ROSAT 0.5 – 2 keV band (indicated by the length of the line) derived by Reynolds & Fabian (1996). Optical data points are from this paper. H_0 = 75, q_0 = 0.0 and z=0.057 have been assumed and no K-correction has been applied.

disk. Accretion directly from the interstellar medium can be neglected as a viable source of double radio lobe power. For a further discussion, see Rees & Saslaw (1975). It would also be very important to locate the X-ray sources more accurately in order to be able to determine their relation to the optical and radio emission.

4.2. Optical emission from the hotspots

Our observations and the HST archive images show optical emission likely to be associated with the radio hotspots B and D. Here we will discuss the implications of this observation shortly.

In Fig. 6 we show the spectra of hotspots A, B and D from radio to X-ray frequences. As already noted by Harris et al. (1994), the X-ray flux densities near hotspots A and D are much higher than what is expected from an extrapolation from the radio-optical data. This means that if the X-rays are coming from the hotspots some mechanism for reacceleration of electrons must exist in the hotspots. The first order Fermi acceleration was invoked by Meisenheimer et al. (1989) as a plausible acceleration process to account for optical emission in the hotspots of radio galaxies. This process operates at the thin shock front moving outwards from the galaxy at the end of the jet. The electrons are scattered across the shock front several times by the influence turbulence and Alfvén waves gaining energy during each cycle. Above certain electron energy E_c the acceleration gain is compensated by the synchrotron losses and the emitted spectrum "cuts off" at a frequency ν_c . The relation between ν_c and observable parameters is given by Meisenheimer et al. (1989) :

$$B_+ = 67\mu\mathrm{G}\left(1-\frac{2}{3}\alpha_0\right)^{-2/3}\times$$
$$u_+^{2/3}L_{\mathrm{kpc}}^{-2/3}\left(\frac{\gamma_c}{\gamma_b}-1\right)^{2/3}\left(\frac{\nu_c}{10^{14}\mathrm{Hz}}\right)^{-1/3} \quad (7)$$

Here B is the magnetic flux density, α_0 is the spectral index below the break frequency ν_b above which the spectrum steepens by $\Delta\alpha$ = -0.5, u is the jet speed relative to speed of light, L is the length of the emission region behind the shock front and $\gamma_c/\gamma_b = \sqrt{\nu_c/\nu_b}$. Negative and positive subscripts refer to upstream and downstream values, respectively. In Fig. 6 the cutoff frequency ν_c of hotspot D would seem to be near 10^{14} Hz assuming that the spectrum retains the same power-law index from radio to infrared frequencies. Using α_0 = -0.5, u_+ = 0.09 and ν_b = 6.5 GHz (Carilli et al. 1991) and L = 2 kpc and $\nu_c = 1\times 10^{14}$ Hz we obtain B = 170 μG in hotspot D. This is close to the range of minimum energy fields B_{me} = 250–350 μG calculated by Carilli et al. (1991) for hotspots in Cygnus A. The hotspots studied by Meisenheimer et al. (1989) have also their magnetic fields close to the minimum energy field. A reasonable estimate for the magnetic field is therefore obtained by assuming that the optical emission from hotspot D is emerging from electrons radiating near the cutoff energy E_c. Another possibility is that the optical (and X-ray) emission is produced by the synchrotron self-compton (SSC) emission (Harris et al. 1994). At hotspot A, for instance, we would expect optical emission with V $\sim$ 25 if B = 300 μG, which is difficult to detect due to the presence of stars W4–W6 if the emission is spread out in a diffuse region. The cutoff frequency ν_c would then be at a frequency $< 10^{14}$ Hz for this hotspot. Deeper observations at many bands are needed in order to study the origin of optical emission in the hotspots of Cygnus A. First, however, the synchrotron origin of the optical emission near hotspots B and D (and possibly A) should be tested by polarimetric observations.

If the optical emission from hotspot B is really synchrotron radiation, there has to be some process responsible for reacceleration here too. If hotspot B is the point where the jet from the nucleus initially hits the intergalacic medium and from there flows towards hotspot A (Williams & Gull 1985), the geometry of the jet flow and physical conditions are expected to be very different from those in the terminal hotspot A. It is therefore not clear if the reacceleration processes invoked to explain the optical emission in the (in our terminology) A hotspots are applicable to the the B hotspots. In the twin jet model this problem does not arise since both hotspots are end points of a jet and the same mechanism is expected to operate in both of them.

5. Summary

We have carried out deep optical imaging and spectroscopy in the radio lobes of Cygnus A to search for accretion disks surrounding supermassive black holes which have been ejected from the nucleus after few-body encounters there (Mikkola &

Valtonen 1990). Motivation to this study comes from the detection of two X-ray point sources close to the radio hotspots by Harris et al. (1994).

Our spectroscopy of the stellar objects at the most probable position shows them to be galactic stars. The BVRI colors of the rest of stellar objects close to radio hotspots are also consistent with them being galactic stars. Optical upper limits $V \gtrsim 25.4$ and $R \gtrsim 24.4$ are derived for an accretion disk to remain undetected in our observations. The limits are sensitive enough to rule out the existence of a full scale accretion disks inside the radio lobes. However, since the outer parts of the accretion disks are stripped away during the close encounters in the nucleus of the galaxy (Lin & Saslaw 1977), the spectrum of the accretion disk can be quite different from the standard full scale disk and the lack of optical emission at the level derived in this paper is not necessarily fatal to the model. Normally in accretion disks the outer parts of the disk contribute most to the optical emission but since they are lost during the ejection process only the X-ray emitting inner parts are left. The subsequent evolution of the disk is unknown, however, and no estimates of the possible range of black hole masses and other parameters can be made before more work is done.

We also detect weak optical emission coinciding with radio hotspots B and D. The synchrotron origin of this optical radiation should be checked with polarimetric observations. The assumption that the optical light in hotspot D is indeed synchrotron radiation leads to an estimate of the cutoff frequency of $\sim 10^{14}$ Hz from which we derive a magnetic flux density B = 170 μG. This is close to the range of minimum energy fields B_{me} = 250–350 μG calculated by Carilli et al. (1991) and is in accordance with Meisenheimer et al. (1989) who also found the magnetic flux density to be close to the equipartition value in a sample of hotspots.

Acknowledgements. The authors thank B. Boyle for obtaining the spectrum of W3. Part of the observations were obtained during RGO service time. The authors thank also the anonymous referee, whose comments clarified the paper. This work has been supported by the Academy of Finland.

References

Arnaud, K.A., Fabian, A.C., Eales, S.A., Jones, C., Forman, W., 1984, MNRAS, 211, 981
Begelman, M.C., Cioffi, D.F., 1989, ApJ, 345, L21
Bessell, M.S., 1979, PASP, 91, 589
Best, P.N., 1996, Vistas in Astronomy, 40, 185
Blandford, R.D., Rees, M.J., 1974, MNRAS, 165, 395
Carilli, C.L., Barthel, N., Diamond, P., 1994, AJ, 108, 64
Carilli, C.L., Barthel, P.D., 1996, A&AR, 7, 1
Carilli, C.L., Dreher, J.W., Conner, S., Perley, R.A., 1989, AJ, 98, 513
Carilli, C.L., Dreher, J.W. and Perley, R.A., 1989, in Hot Spots in Extragalactic Radio Sources, eds. K. Meisenheimer and H.J. Röser, Berlin – Springer, p. 51
Carilli, C.L., Perley, R.A., Dreher, J.W., Leahy, J.P., 1991, ApJ, 383, 554
Carilli, C.L., Perley, R.A., Dreher, J.H., 1988, ApJ, 334, L73
Clegg, R., Carter, D., Charles, P. et al., 1992, ISIS astronomers' guide, RGO user manual
Cox, C.I., Gull, S.F., Scheuer, P.A.G., 1991, MNRAS, 252, 558
De Young, D.S., 1977, ApJ, 211, 329
Hargrave, P.J., Ryle, M., 1974, MNRAS, 166, 305
Harris, D.E., Carilli, C.L., Perley, R.A., 1994, Nat, 367, 713
Howell, S.B., 1992, in Astronomical CCD Observing and Reduction Techniques, ASP Conference Series, Ed. S.B. Howell, Vol 23, p. 105
Irwin, M., Maddox, S., McMahon, R., 1994, Spectrum, 2, 14
Koide, S., Sakai, J.-I., Nishikawa, K.-I., Mutel, R.L., 1996 ApJ, 464, 724
Krichbaum, T.P., Witzel, A., Graham, D.A. et al., 1993, A&A, 275, 375
Kauffmann, G., White, S.D.M., 1993, MNRAS, 261, 921
Kronberg, P., van den Bergh, S., Button, S., 1977, AJ, 82, 315
Lin, D.N.C., Saslaw, W.C., 1977, ApJ, 217, 958
Landolt, A.U., 1983, AJ, 88, 439
Landolt, A.U., 1992, AJ, 104, 340
Lonsdale, C.J., Barthel, P.D., 1986, AJ, 92, 12
Meisenheimer, K., Röser, H.-J., 1986, Nat, 319, 459
Meisenheimer, K., Röser, H.-J., Hiltner, P.R. et al., 1989, A&A, 219, 63
Meisenheimer, K., 1992, in Physics of Active Galactic Nuclei, eds. W.J. Duschl and S.J. Wagner, Berlin – Springer, p. 525
Mikkola, S., Valtonen, M.J., 1990, ApJ, 348, 412
Muxlow, T.W.B., Pelletier, G., Roland, J., 1988, A&A, 206, 237
Norman, M.L., 1989, in Hotspots in Extragalactic Radio Sources, eds. K. Meisenheimer and H.-J. Röser, Heidelberg – Springer, p. 193
Perley, R.A., Carilli, C.L., 1996, in "Cygnus A: Study of a Radio Galaxy", eds. C.L. Carilli and D.L. Harris, Cambridge – Cambridge University Press
Perley, R.A., Dreher, J.W., Cowan, J.J., 1984, ApJ, 285, L35
Perley et al., 1997, in preparation
Rees, M.J., Saslaw, W.C., 1975, MNRAS, 171, 53
Reynolds, C.S., Fabian, A.C., 1996, MNRAS, 278, 479
Röser, H.-J., 1989, in Hotspots in Extragalactic Radio Sources, eds. K. Meisenheimer and H.-J. Röser, Heidelberg – Springer, p. 91
Savage, B.D., Mathis, J.S., 1979, ARA&A, 17, 73
Sakura, N.I, Sunyaev, R.A., 1973, A&A, 24, 337
Scheuer, P.A.G., 1982, in Extragalactic Radio Sources, IAU Symp. 97, eds. D.S. Heeschen and C.M. Wade, Dordrecht – Reidel, p. 163
Stetson, P.B., 1987, PASP, 99, 191
Thompson, R.J., 1995, ApJ, 454, 660
Valtaoja, E., 1984, A&A, 140, 148
Valtonen, M.J., 1979, ApJ, 227, L79
Valtonen, M.J., 1996, Comments Astrophys., 18, 191
Valtonen, M.J., Mikkola, S., Heinämäki, P., Valtonen, H., 1994, ApJS, 95, 69
Wandel, A., Liang, E.P., 1991, ApJ, 380, 84
Wandel, A., Petrosian, V., 1987, in Active Galactic Nuclei, Proceedings of a conference held at the Georgia State University, eds. H.R. Miller and P.J. Wiita, Berlin – Springer, p. 225
Wandel, A., Petrosian, V., 1988, ApJ, 329, L11
Wandel, A., Urry, C.M., 1991, ApJ, 367, 78
Williams, A.G., Gull, S.F., 1984, Nat, 310, 33
Williams, A.G., Gull, S.F., 1985, Nat, 313, 34

This article was processed by the author using Springer-Verlag LaTeX A&A style file *L-AA* version 3.